Review

Structural bioinformatic analysis of DsbA proteins and their pathogenicity associated substrates

Carlos Santos-Martin [a,1], Geqing Wang [a,1], Pramod Subedi [a], Lilian Hor [a], Makrina Totsika [b], Jason John Paxman [a,*], Begoña Heras [a,*]

[a] Department of Biochemistry and Genetics, La Trobe Institute of Molecular Science, La Trobe University, Melbourne, Australia
[b] Centre for Immunology and Infection Control, School of Biomedical Sciences, Queensland University of Technology, Brisbane, Australia

ARTICLE INFO

ABSTRACT

The disulfide bond (DSB) forming system and in particular DsbA, is a key bacterial oxidative folding catalyst. Due to its role in promoting the correct assembly of a wide range of virulence factors required at different stages of the infection process, DsbA is a master virulence rheostat, making it an attractive target for the development of new virulence blockers. Although DSB systems have been extensively studied across different bacterial species, to date, little is known about how DsbA oxidoreductases are able to recognize and interact with such a wide range of substrates. This review summarizes the current knowledge on the DsbA enzymes, with special attention on their interaction with the partner oxidase DsbB and substrates associated with bacterial virulence. The structurally and functionally diverse set of bacterial proteins that rely on DsbA-mediated disulfide bond formation are summarized. Local sequence and secondary structure elements of these substrates are analyzed to identify common elements recognized by DsbA enzymes. This not only provides information on protein folding systems in bacteria but also offers tools for identifying new DsbA substrates and informs current efforts aimed at developing DsbA targeted anti-microbials.

© 2021 The Authors. Published by Elsevier B.V. on behalf of Research Network of Computational and Structural Biotechnology. This is an open access article under the CC BY-NC-ND license (http://creativecommons.org/licenses/by-nc-nd/4.0/).

Contents

* Corresponding authors.
  E-mail addresses: j.paxman@latrobe.edu.au (J.J. Paxman), b.heras@latrobe.edu.au (B. Heras).
[1] Both authors contributed equally to this work

1. Introduction

Bacteria rely on the production of a wide range of virulence factors to adapt to different environments, surpass host immune responses and colonize and invade host cells [1–3]. These virulence factors are often secreted or cell surface proteins that include disulfide bonds (DSB) in their three-dimensional structures, which provide stability in the hostile, protease-rich extracellular environment [4,5]. Disulfide bonds are catalyzed by the disulfide bond forming enzyme A (DsbA) of the DSB system in a process known as oxidative protein folding [4,5]. The discovery of DsbA (*Ec*DsbA) within the periplasmic space of *Escherichia coli*, provided the first experimental basis for a catalytic mechanism of disulfide bond formation in Gram-negative bacteria [6]. The reliance on this disulfide bond formation machinery for the correct functioning of several bacterial proteins, including virulence factors, has been directly shown in a number of *in vitro* and cell-based assays [7]. Furthermore, several studies have demonstrated that mutants defective in the DSB oxidative folding pathway throughout diverse bacterial pathogens, have reduced virulence phenotypes in animal infection models [6,8–19]. Since the discovery of the DSB system in *E. coli* K-12, the study of these systems has been expanded to include diverse Gram-negative and Gram-positive bacteria [4,5,20–22]. However, how this important DSB forming enzyme interacts with a great array of structurally diverse protein substrates is still poorly understood. In this review we summarize current knowledge on DsbA systems, particularly focusing on how DsbA proteins interact with partner oxidases and virulence substrates. Through an extensive bioinformatic analysis we define common features present in the highly diverse set of DsbA substrates.

1.1. The archetypal DSB machinery in prokaryotes

The DSB system was first characterized and has been best studied in the Gram-negative bacterium *Escherichia coli* K-12 [6]. This prototypical DSB system consists of two different pathways: (i) The DSB oxidation pathway (Fig. 1A), where the oxidoreductase enzyme DsbA introduces disulfide bonds between consecutive cysteines in unfolded substrates as they are translocated into the periplasm [6]; and (ii) the DSB isomerization pathway (Fig. 1B), where non-native disulfide bonds are proofread and corrected [23,24] by the isomerase enzyme DsbC [25]. For each one of these pathways, the active oxidized state of DsbA and the active reduced state of DsbC are maintained by the proteins DsbB and DsbD, respectively [7,26–29]. DsbB is an integral membrane protein with two periplasmic loops, each containing two pairs of redox active cysteines required for DsbA re-oxidation. DsbD is a multidomain membrane protein with two periplasmic domains flanking a transmembrane domain. These membrane proteins display high substrate specificity for DsbA and DsbC, respectively, allowing for both opposite redox pathways to function independently in the shared periplasmic compartment.

2. The thiol oxidase DsbA from *E. coli* K-12

*Ec*DsbA, as revealed by its crystal structure, is composed of two domains: a thioredoxin (TRX) domain, and a helical domain (Fig. 2A) [30]. The TRX domain consists of four β-strands and two α-helices (β₂α₁β₃ and β₄β₅α₇ motif), a structural scaffold characteristic of disulfide oxidoreductases, while the helical domain (α₂-α₆), which is inserted within the TRX domain, is comprised of five α-helices (a three-helical bundle with two additional helices). The active site of *Ec*DsbA siting within the TRX domain is composed of a conserved CXXC motif (Cys30-Pro31-His32-Cys33). With an unusually low pK_a of 3.5 [31], the N-terminal Cys30 exists as a thi-
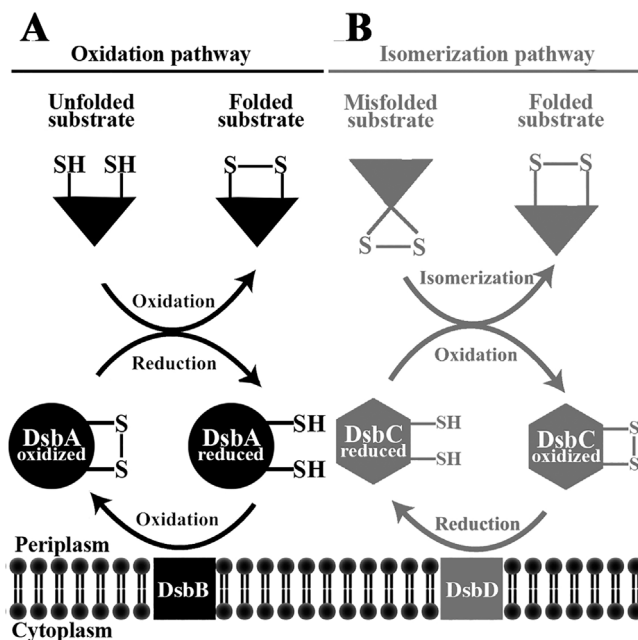

Fig. 1. The DSB machinery in *E. coli* K-12. A. DsbA/B oxidative pathway. Unfolded cysteine-containing proteins are oxidized by the periplasmic protein DsbA, which is reduced during this process and is in turn re-oxidized by the inner membrane protein DsbB. B. DsbC/D isomerization pathway. DsbC proofreads and re-shuffles non-native disulfide bonds in misfolded substrates. The inner membrane protein DsbD maintains DsbC in its reduced form in the oxidizing periplasmic environment.

olate ion in the reduced form at physiological pH. This Cys30 thiolate is stabilized by a number of polar interactions such as (i) a hydrogen bond with the thiol of Cys33 (ii) hydrogen bonds with the backbone amide nitrogens of Cys30 and His32; and (iii) electrostatic interactions with the side chain of His32 [32]. Additionally, the partial positive charge from the dipole of the α1 helix, where the active site is located, has also been suggested to stabilize the Cys30 thiolate [32]. This results in superior stability of the reduced form of DsbA and a stronger tendency to oxidize substrates. Another key feature of the TRX domain is a *cis*-proline loop (Val-*cis*-Pro), which is spatially close to the active site. This feature is thought to be important for the correct binding of substrates and/or DsbA-substrate complex resolution, along with influencing the redox properties of thioredoxin fold proteins [33–35] (Fig. 2A). Examination of *Ec*DsbA's electrostatic surface shows a hydrophobic groove present in the TRX domain (Fig. 2A), which has been shown to interact with its cognate membrane partner *Ec*DsbB [27,30,36]. Similarly, the surface of the *Ec*DsbA helical domain forms a large hydrophobic patch located immediately above the active site (Fig. 2A). This patch has been shown to interact with substrates and is thought to provide stability and specificity for substrate binding [36]. The hydrophobic nature of the surface surrounding the active site is consistent with its ability to catalyze folding of a broad range of unfolded or partially folded substrates along with interacting with the periplasmic loop of DbsB [4,24,36–38].

2.1. Diversity of DsbA oxidative proteins across bacteria

DSB systems are widespread across non-pathogenic and pathogenic bacteria [4,5] and the characterization of DSB systems and DsbA enzymes across diverse species has revealed structural and active site differences within the DsbA family of proteins [20]. A combined structural and bioinformatics analysis highlighted that the most notable of these differences is the arrangement of the β-strand (β1) preceding the TRX domain, which divides DsbAs into

two major classes, class I with β-sheet topology of 3–2–4–5–1 (Fig. 2A and B) and class II with a topology of 1–3–2–4–5 (Fig. 2C and D), throughout most Gram-negative and Gram-positive bacteria [39]. These classes are further split into the Ia, Ib, IIa and IIb subclasses based on variations of surface features surrounding their active sites [39]. The canonical EcDsbA is grouped into class Ia (Fig. 2A), which also includes DsbA proteins from other important human pathogens such as *Salmonella enterica* serovar Typhimurium (*Se*), *Klebsiella pneumoniae* (*Kp*), *Vibrio cholerae* (*Vc*) and *Proteus mirabilis* (*Pm*) [40]. DsbA proteins from this class share an extended hydrophobic groove adjacent to the active site mapping at the β4β5α7 region of the TRX domain (Fig. 2A), that is involved

in the interaction with DsbB for reoxidation [27]. The same groove is shorter in members of class Ib such as *Burkholderia pseudomallei* (*Bps*DsbA) (Fig. 2B) [39]. Consistent with the similarity between DsbA proteins from class Ia, it has been found that other class Ia DsbAs such as *Se*DsbA, *Kp*DsbA, *Vc*DsbA and *Pm*DsbA can fully complement *Ec*DsbA *in vitro* and *in vivo* [40–44], while DsbA proteins from class Ib such as *Bps*DsbA and *Pseudomonas aeruginosa* (*Pa*) DsbA can only partially complement *Ec*DsbA [17,45]. Class II DsbA proteins, such as *Staphylococcus aureus* (*Sa*DsbA) and *Wolbachia pipientis* (*Wp*DsbA1), further deviate from the canonical *Ec*DsbA by featuring the most truncated hydrophobic groove and a highly charged electrostatic surface surrounding the active site (Fig. 2C, 2D) [39]. Unsurprisingly, among the four structurally characterized class II DsbAs, only *Sa*DsbA is able to partially restore *Ec*DsbA activity *in vivo* [46]. A more recent analysis investigating the phylogenetic relationship of 20 structurally characterised DsbA homologues from diverse bacteria, assigned DsbA proteins into three main clades, with the first and second being equivalent to previously defined class Ia and class Ib DsbAs [39], and the third more taxonomically diverse clade consisting of structurally divergent *Ec*DsbA proteins [47].

In addition to being structurally diverse, there is also significant divergence in the redox properties of DsbA-like proteins (Table 1). For instance, DsbA1 from *Neisseria meningitidis* (*Nm*) has a redox potential of −79 mV and a pK_a of 3.0 for the N-terminal nucleophilic cysteine [48]. In contrast, DsbA1 from *W. pipientis* (*Wp*DsbA1) is much less oxidizing with a redox potential of −163 mV and a pK_a of 4.7 [49]. Previous studies have demonstrated that the XX dipeptide sequence in the active site CXXC motif and the residue preceding the *cis*-Pro motif modulate these redox potentials and pK_a of the N-terminal nucleophilic cysteine [34,50]. However, these motifs are not the sole determinants of the redox properties. For example, *Bps*DsbA and *Pa*DsbA share the same CPHC motif and Val-*cis*-Pro sequence as the *Ec*DsbA, but they are more oxidizing ($E^{o'}$−94 mV) than EcDsbA ($E^{o'}$-−122 mV) and display lower pK_a values of the nucleophilic cysteine. Overall, variations in the active site sequence, three-dimensional structure, surface charge and redox characteristics collectively contribute to the unique features of each DsbA and likely define their substrate specificities [35].

2.2. Functional redundancy of DsbA homologues

Genome-wide screening for DSB homologues has revealed that the classical model of bacterial oxidative folding from *E. coli* K-12 is
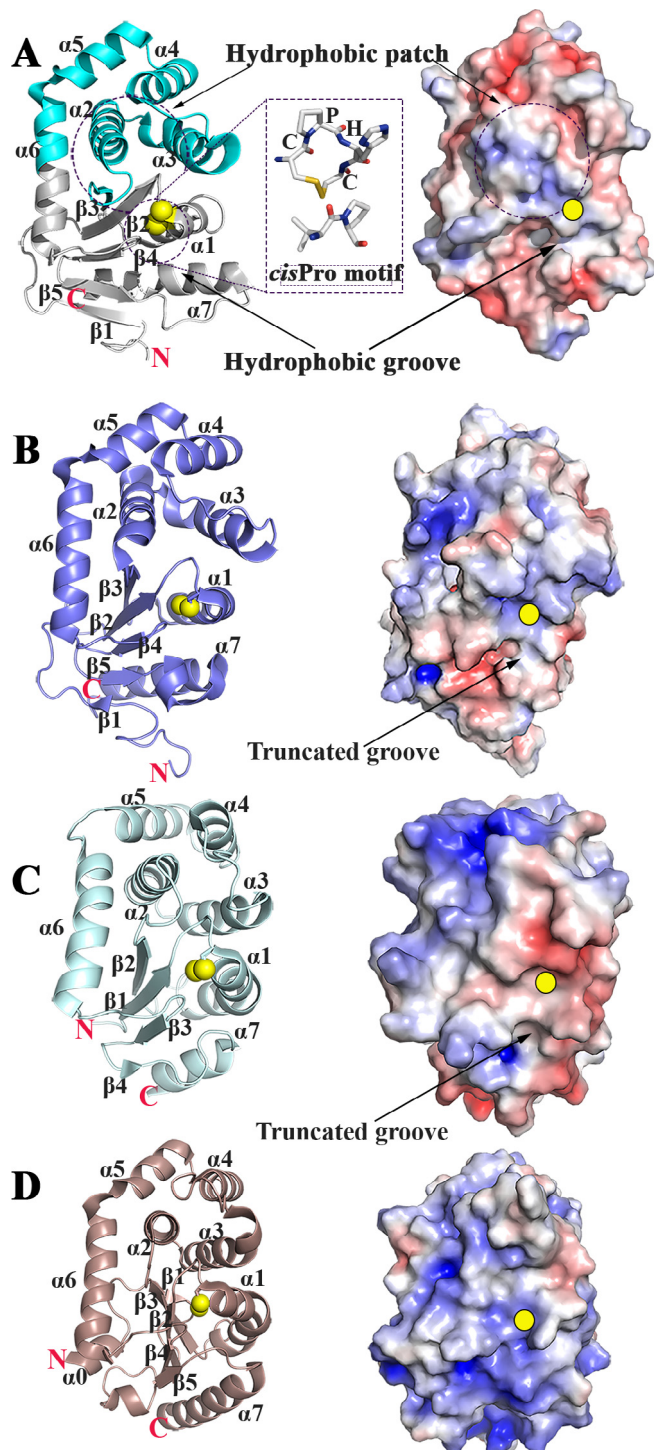

Fig. 2. Structural variation of DsbA proteins across bacteria. A. Cartoon representation (left) of *E. coli* *Ec*DsbA (PDB ID: 1FVK) (subclass Ia) showing the thioredoxin (TRX) domain (white), α-helical domain (cyan) and sulfur atoms of the active site cysteine residues (yellow). Secondary structure elements are indicated. Inset shows the close-up view of the *Ec*DsbA catalytic site with the characteristic CXXC catalytic motif (Cys-Pro-His-Cys) and Val-*cis*-Pro motif. B. Cartoon representation (left) and electrostatic surface representation (right) of *B. pseudomallei* *Bps*DsbA (subclass Ib) (PDB ID: 4K2D). *Bps*DsbA has a more truncated groove adjacent to the active site relative to that of *Ec*DsbA due to a deletion in α7 and the loop connecting α7 and β5. C. Cartoon representation (left) and electrostatic surface representation (right) of *S. aureus* *Sa*DsbA (subclass IIa) (PDB ID:3BCI). *Sa*DsbA displays a more truncated groove relative to that of *Bps*DsbA due to a substantial deletion in α7 and the loop connecting α7 and β4. The surface close to the active site is negatively charged. D. Cartoon representation (left) and electrostatic surface representation (right) of *W. pipientis* *Wp*DsbA1 (subclass IIb) (PDB ID:3F4R). *Wp*DsbA1 does not have a well-defined groove and features a positively charged surface adjacent to the active site. Electrostatic surface potential is contoured between −5 (red) and +5 (blue) kT/e. The hydrophobic grooves and hydrophobic patch are indicated with black arrows. The active site in the electrostatic representation is indicated as a yellow circle. (For interpretation of the references to colour in this figure legend, the reader is referred to the web version of this article.)

Table 1
Summary of redox properties of DsbA proteins across bacteria.

Organism	Protein name	CXXC	$E^{o'}$ (mV)	pK$_a$	Ref
E. coli K-12	DsbA	CPHC	−122	3.4	[30,31]
V. cholerae	DsbA (TcpG)	CPHC	−116	–	[43,51]
S. aureus	DsbA	CPYC	−132	3.4	[46,52]
X. fastidiosa	DsbA	CPHC	−94	–	[53]
UPEC CFT073	DsbL	CPFC	−95	–	[54]
W. pipientis wMel	DsbA1	CYHC	−163	4.7	[49]
N. meningitidis MC58	DsbA3	CVHC	−87	–	[48,55]
	DsbA1	CPHC	−89	3	[48,55]
Bacillus subtilis 168	DsbA (BdbD)	CPSC	−80	~3.5	[56]
P. aeruginosa	DsbA	CPHC	−94	–	[45]
S. enterica Typhimurium *SL1344*	SrgA	CPPC	−154	4.7	[41]
	DsbA	CPHC	−126	3.3	[41]
	DsbL	CPFC	−97	3.8	[41]
	BcfH	CSWC	−101, −151	–	[57]
B. pseudomallei	DsbA	CPHC	−92	2.83	[17]

not universally conserved across bacterial species [4,58]. Bioinformatic and functional studies have revealed that many bacteria encode more than one DsbA [4,5,19]. Examples include uropathogenic *E. coli* (UPEC) strain CFT073 that possesses a canonical DsbA and an accessory DsbA homologue DsbL [19,54] or the widely distributed facultative anaerobe *Shewanella oneidensis*, which has a complex DSB machinery with four DsbA (DsbA1-4) and two DsbB (DsbB1-2) homologues [59]. Similarly, *Salmonella enterica* (*Se*) encodes four DsbA-like proteins [41], namely DsbA, DsbL, SrgA [42], a virulence plasmid-encoded DsbA-like protein, and ScsC [60,61], a DsbA-like protein that protects against copper toxicity [57,62]. These *Salmonella* DsbA paralogues were found to share low sequence identity along with significant differences in their surface features and redox properties [41]. More recently, a novel DSB-like protein from *Salmonella enterica* termed BcfH has been identified and characterized. Interestingly, BcfH has been shown to form a trimeric structure, exceptionally uncommon among the thioredoxin superfamily members. Additionally, BcfH has both thiol oxidase and disulfide isomerase activities contributing to *Salmonella* fimbrial biogenesis [57].

Based on current published evidence, it appears that in bacteria with multiple DsbA homologues, there is always one homologue that acts as the primary disulfide donor capable of oxidizing a wide range of substrates, whilst other DsbAs are dedicated for specific substrates [5]. While many bacteria possess an extended collection of accessory DsbA homologues with differing specificities to catalyze the oxidation of selective substrates [4], some DsbA homologues have shown a level of functional redundancy. Such is the case of UPEC DsbL (*Ec*DsbL) that possesses a positively charged surface surrounding the active site that serves as a specific oxidase of the periplasmic protein arylsulfate sulfotransferase (ASST) [54]. The *astA* gene is a UPEC-associated gene and its expression is upregulated during urinary tract infections. Although less oxidizing in nature than *Ec*DsbL ($E^{o'}$−95 mV), *Ec*DsbA ($E^{o'}$−120 mV) has also been found to oxidize ASST at a similar rate *in vitro* [63]. Conversely, it has also been observed that *Ec*DsbL can partially complement *Ec*DsbA *in vivo* [19,54]. Similarly, DsbA homologues from the pathogen *Salmonella enterica* serovar Typhimurium, *Se*DsbA, *Se*SrgA and *Se*DsbL, are all able to complement each other in restoring bacterial motility and plasmid-encoded fimbriae (Pef) production *in vivo* [41], irrespective of sharing low sequence identity and having considerably different redox potentials ($E^{o'}$ of −126 mV, −154 mV and −97 mV, respectively) [41]. Despite this functional redundancy, the flagella system is considered a substrate of *Se*DsbA, and PefA a substrate of *Se*SrgA [42]. Although it is still not fully understood why some bacterial genomes encode multiple and functionally redundant DsbA homologues, one possibility could be that under a given set of growth conditions, a single type

of DsbA is insufficient to drive efficient oxidative folding. This hypothesis seems to be supported by the co-expression of virulence factors and their specific oxidases as it has been seen with DsbL/ASST and SrgA/PefA [42,54].

3. The redox interaction between DsbA and DsbB

The systematic oxidation of substrates in the periplasm by DsbA proteins largely relies on the efficient reoxidation of the enzyme by the membrane embedded protein DsbB [27]. Due to the fast-resolving nature of the mixed disulfide formed between DsbA and DsbB (Fig. 3), it has been particularly challenging to study this interaction at the atomic level. However, a study involving the active site mutant Cys33Ala of *Ec*DsbA was able to successfully trap *Ec*DsbB in a disulfide-linked intermediate form [27]. This hallmark crystal structure of the intermediate complex offered for the first time, molecular insights into the protein–protein interaction between DsbA and DsbB (PDB ID: 2HI7, 2ZUP) [27,64], confirming the formation of a mixed disulfide bond between Cys104 of *Ec*DsbB and the nucleophilic Cys30 of *Ec*DsbA. Additionally, the protein–protein interaction interface was shown to be mediated by the second periplasmic loop of the transmembrane protein *Ec*DsbB (P2). A high shape complementarity is observed between the N-terminal end of the P2 periplasmic loop of *Ec*DsbB (Pro100-Thr103) and the hydrophobic groove of *Ec*DsbA, which is formed by the active site CPHC motif, the *cis*-Pro motif (L2 loop) and L3 loop (Fig. 3A), while the other end of the P2 periplasmic loop (Asp105-Phe106) of *Ec*DsbB interacts with the hydrophobic patch of *Ec*DsbA via backbone hydrogen bonds with the L2 loop and hydrophobic interactions with the L1 loop. Overall, the DsbA-DsbB binding interface spans the helical domain and the thioredoxin domain of DsbA. The hinge bending motions of the two domains have been suggested to promote the protein–protein interactions and disulfide bond catalysis [32]. Interestingly, binding of *Ec*DsbB to *Ec*DsbA does not seem to induce major conformational changes in *Ec*DsbA with a root mean square deviation (RMSD) value of 0.788 Å over 176 Cα atoms when overlaid with apo *Ec*DsbA (PDB ID:1FVK) [65], with most of the structural shifts located in flexible loop regions of the protein.

The binding mode of the *Ec*DsbA-*Ec*DsbB interaction was further validated by a crystal structure of *Ec*DsbA Cys33Ala mutant in complex with an optimized heptapeptide (PFATCDS) derived from the P2 loop of *Ec*DsbB [66]. The *Ec*DsbA-peptide complex strongly resembles the interactions observed in the *Ec*DsbA-*Ec*DsbB protein–protein complex (Fig. 3B). Alanine-scanning mutagenesis of the *Ec*DsbB 9-mer P2 based peptide (PSPFATCDF) showed that the cysteine residue (equivalent to Cys104 in *Ec*DsbB), contributed most to the binding affinity with *Ec*DsbA [66], suggest-
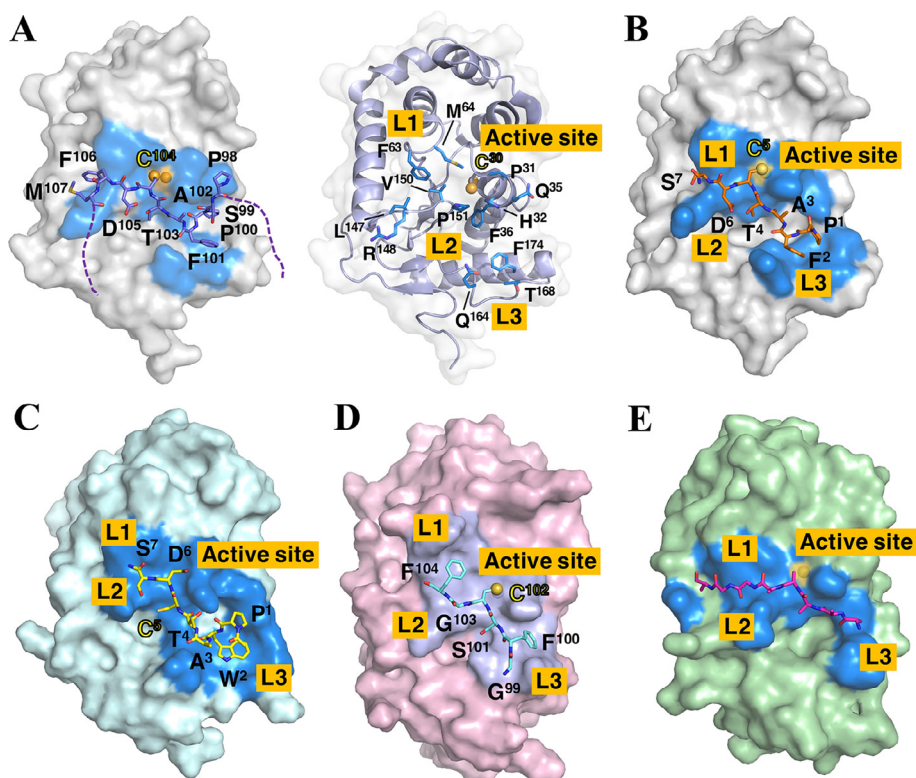
Fig. 3. Interaction between DsbA and DsbB. A. Crystal structure of the *Ec*DsbA-*Ec*DsbB complex (PDB ID: 2ZUP). Only the DsbA-interacting segment of the DsbB periplasmic loop P2 (purple) is shown for clarity. The dashed line indicates the omitted DsbB protein. Left panel: *Ec*DsbA is shown as colored surface, *Ec*DsbA residues located within 4 Å of *Ec*DsbB are shaded in blue. Residue number of *Ec*DsbB is labelled in the figure. Right panel: *Ec*DsbA residues located within 4 Å of DsbB are shown as sticks. Sulfur atoms of the active site cysteines are shown as yellow spheres. Surface loops L1, L2, L3 and CPHC active site are labelled in each structure. B. Crystal structure of *Ec*DsbA in complex with an optimized heptapeptide (PFATCDS) derived from *Ec*DsbB (PDB ID: 4TKY). C. Crystal structure of *Pm*DsbA C30S mutant in complex with an optimized heptapeptide (PWATCDS) from *Pm*DsbB (PDB ID: 4OD7). D. Crystal structure of *Bps*DsbA in complex a *Bps*DsbB-derived peptide (GFSCGF) (PDB ID: 5VYO). E. Crystal structure of *Xf*DsbA in complex with a DsbB-like peptide (PDB ID: 2REM). For B-E, DsbA is shown as colored surface, DsbA residues located within 4 Å of DsbB are shaded in blue. Sulfur atoms of the active site cysteines are shown as yellow spheres. (For interpretation of the references to colour in this figure legend, the reader is referred to the web version of this article.)

ing that the peripheral hydrophobic interactions may only serve to specifically recognize *Ec*DsbB and position the cysteine in the correct orientation for disulfide bond formation.

Despite the structural variation amongst DsbA homologues and the low sequence conservation in residues at the DsbB binding interface, the characterized DsbA-DsbB peptide complexes from different bacteria have shown a conserved binding site, which spans across the DsbA hydrophobic patch and hydrophobic groove adjacent to the active site (Fig. 3B-E). Indeed, a study on *Proteus mirabilis* DsbA (*Pm*DsbA) Cys30Ser mutant co-crystallized with an optimized heptapeptide derived from the P2 periplasmic loop of *Pm*DsbB (PWATCDS) [40] showed that although the peptide does not form the mixed disulfide with *Pm*DsbA, the binding mode is strikingly similar to that of the *Ec*DsbA-*Ec*DsbB complex. This complex also supports the significance of the non-disulfide interactions in DsbB binding (Fig. 3C). Similarly, a complex between *Bps*DsbA, a distant homologue of *Ec*DsbA with a truncated hydrophobic groove, and a *Bps*DsbB-derived peptide showed the peptide binding to *Bps*DsbA in a very similar manner to its *E. coli* counterpart (Fig. 3D) [20,67]. These findings, in addition to a crystal structure of *Xylella fastidiosa* (*Xf*) DsbA crystallized with a DsbB-like peptide [53] (Fig. 3E), highlight the conservation of this binding mode across bacterial species. Notably, in these structures, all DsbB peptides form backbone hydrogen bonds with the L2 loop of DsbA, which seems to facilitate the presentation of the cysteine residue for efficient disulfide bond exchange.

Based on observations of the DsbA-DsbB/DsbB-peptide interactions from different Gram-negative bacteria, it is tempting to propose that the conserved DsbB-interacting interface on DsbA

consists of the L1 loop, the active site CXXC motif, the *cis*-Pro motif (L2 loop), and the hydrophobic groove (L3 loop) (Fig. 3). However, since all DsbAs in these characterized complexes belong to class I DsbAs, it remains to be determined whether class II DsbAs interact with DsbB in a similar manner given their more pronounced structural and surface variations.

4. The DsbA-substrate interaction

As part of the oxidative folding process in Gram-negative bacteria, DsbA introduces disulfide bonds into newly synthesized polypeptides immediately after they are translocated into the periplasm through the Sec channel [68]. The DsbA-catalyzed thiol-disulfide exchange reaction appears to proceed via a biomolecular nucleophilic substitution reaction (S_N2) mechanism in two steps (Fig. 4). In the first step, the deprotonated cysteine of the substrate attacks the DsbA Cys30 sulfur atom that is participating in a Cys30-Cys33 disulfide bond. This leads to a DsbA-substrate intermediate complex with a disulfide bond between the DsbA Cys30 and the substrate cysteine. In the second step, a second cysteine in the substrate is deprotonated and attacks the sulfur atom of the substrate cysteine in the mixed disulfide bond, resolving the complex and producing oxidized substrate and reduced DsbA [68–70].

Due to the extremely short-lived nature of the mixed disulfide between DsbA and a substrate, it has been challenging to capture and characterize DsbA-substrate complexes at the atomic level. At present the only two structurally characterized DsbA-substrate peptide complexes offer a glimpse into the molecular determinants underlying the DsbA-substrate interactions. In one
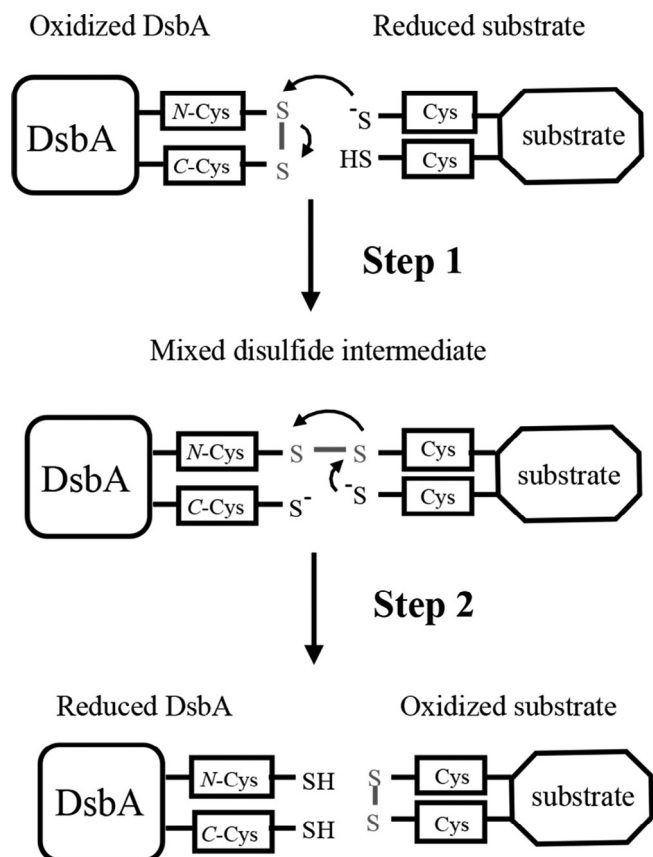
Fig. 4. *Ec*DsbA-catalyzed substrate oxidation. This thiol-disulfide exchange reaction is understood to proceed via a biomolecular nucleophilic substitution reaction (S_N2) mechanism involving the attack of the deprotonated cysteine of the substrate to the DsbA Cys30 sulfur atom involved in the Cys30-Cys33 disulfide bond. This leads to the formation of the DsbA-substrate intermediate complex. In the second step, a second cysteine in the substrate is deprotonated and attacks the sulfur atom of the substrate cysteine in the mixed disulfide bond, resolving the complex and producing oxidized substrate and reduced DsbA *N*-Cys refers to *N*-terminal cysteine of the active site CXXC motif, *C*-Cys refers to *C*-terminal cysteine of the active site CXXC motif.

Fig. 5. Crystal structures of the DsbA-substrate complexes. A. Crystal structure of *Ec*DsbA in complex with an autotransporter SigA-derived peptide. (PDB ID: 3DKS). Left panel: DsbA is shown as colored surface, *Ec*DsbA residues located within 4 Å of the SigA peptide are shaded in blue. Residue number of the SigA peptide is labelled in the figure. Right panel: *Ec*DsbA residues located within 4 Å of *Ec*DsbB are labelled and shown as purple sticks. Sulfur atoms of the active site cysteines are shown as yellow spheres. Surface loops L1, L2, L3 and CPHC active site are labelled. B. Crystal structure of *Ab*DsbA in complex with *E. coli* elongation factor EF-Tu (PDB ID: 4P3Y). Only the *Ab*DsbA-interacting segment of EF-Tu is shown for clarity. Left panel: catalytic face of *Ab*DsbA, sulfur atoms of the active site cysteines are shown as yellow spheres. Right panel: non-catalytic face of *Ab*DsbA. DsbA is presented as grey surface, DsbA residues located within 4 Å of EF-Tu are shaded in blue. (For interpretation of the references to colour in this figure legend, the reader is referred to the web version of this article.)

study, a peptide derived from the autotransporter protein SigA of *Shigella flexneri* was trapped in a complex with *Ec*DsbA by substituting the native cysteine of the peptide with a homoserine (Hse) [36,71]. This modification allowed for the formation of a stable complex through a non-labile covalent bond between the Hse of the peptide and the reactive Cys30 of *Ec*DsbA. The crystal structure of the complex revealed that the SigA peptide mainly interacts with the active site and the hydrophobic patch (L1, L2 loops) of DsbA (Fig. 5A). This interaction is comparable with that displayed by the DsbA-DsbB complexes, where the binding site of the substrate also spans the helical domain and thioredoxin domain, and where the backbone hydrogen bonds between the L2 loop of DsbA and the N-terminal segment of SigA peptide (Hse6-Gln7-Lys8) mimic the interactions in the DsbA-DsbB complexes, suggesting a conserved DsbA-substrate recognition mechanism. However, unlike DsbB, the C-terminal segment of the SigA peptide does not extend into the hydrophobic groove below the active site but instead sits on the top of it. Interestingly, the lack of interactions between Cys30 and His32 in the mixed intermediate, allows the sidechain of the His32 to be less constrained where in the case of the SigA peptide, it forms π-π stacking interactions between the Phe4 of the peptide and His32 of DsbA (Fig. 5A).

In another study, the crystal structure of *Acinetobacter baumannii* DsbA (*Ab*DsbA) in complex with the *E. coli* elongation factor EF-
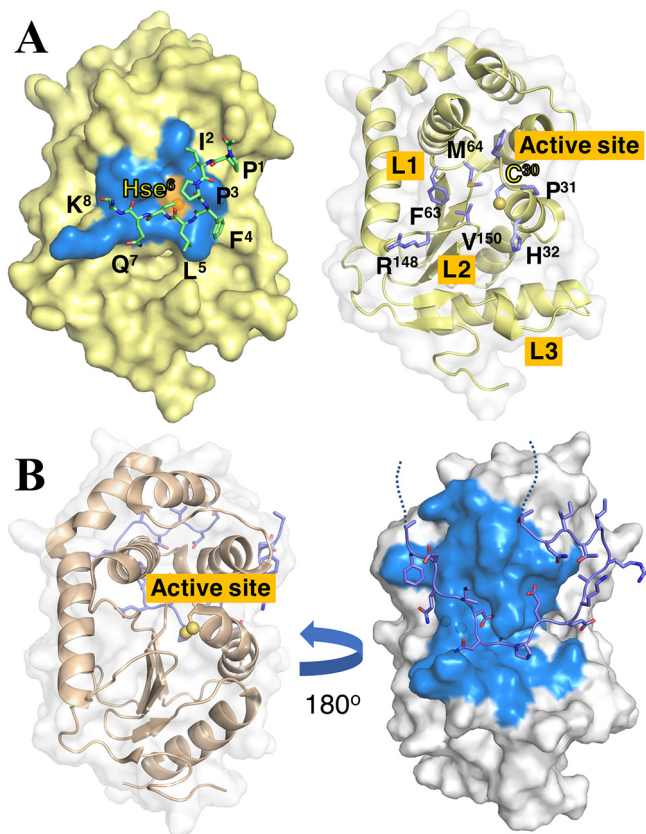
Tu uncovered a very uncommon substrate binding region that does not involve the disulfide exchange reaction [72]. For this complex, EF-Tu binds tightly to a groove sandwiched between the thioredoxin domain and the helical domain on the non-catalytic face of *Ab*DsbA (Fig. 5B). Although the activity of *Ab*DsbA is shown to be reduced in the presence of *Ec*EF-Tu *in vitro* (*E. coli* and *A. baumannii* EF-Tu share 85% sequence identity), the physiological relevance of this allosteric interaction is still unclear.

5. Structural variability of DsbA substrates

Compared to DsbA proteins, DsbA substrates are highly variable and structurally less conserved [44]. The identification of potential DsbA substrates has been made possible by using (i) two dimensional gel electrophoresis to compare wild type and Δ*dsb*A strains; (ii) substrate trapping by modification of the C-terminal cysteine present in the active site of DsbA proteins or (iii) mutating the *cis*−Pro residue (*cis*−Pro151 in *Ec*DsbA) adjacent to the active site to threonine to trap stable enzyme-substrate intermediate complexes [23,73–75].

Table 2
Structurally characterized DsbA substrates.

Organism	Substrate	PDB code	S–S[a]	Structural location[b]	
				Cys$_1$	Cys$_2$
Bordetella pertussis	S1 subunit	1BCP: chain A	41–202	α-Helix	Loop
Bordetella pertussis	S2 subunit	1BCP: chain B	23–87	Loop	β-Sheet
			120–134	β-Sheet	β-Sheet
			192–199	Loop	Loop
Erwinia chrysanthemi	CelZ	1AIW	4–16	Loop	Loop
Erwinia chrysanthemi	PelC	1AIR	72–155	α-Helix	β-Sheet
			329–352	α-Helix	Loop
Escherichia coli (UPEC)	ASST	3ELQ	418–424	Loop	Loop
Escherichia coli (UPEC)	PapD	3DPA	207–212	Loop	β-Sheet
Escherichia coli (EPEC)	BfpA	1ZWT	94–144	α-Helix	Loop
Escherichia coli (EPEC)	EscC	3GR5	136–155	Loop	α-Helix
Escherichia coli (ETEC)	EltB	1B44	9–86	α-Helix	β-Sheet
Escherichia coli (ETEC)	STb	1EHS	10–48[c]	Loop	Loop
			21–36[c]	α-Helix	Loop
Escherichia coli	YodA	1OEE	103–128	β-Sheet	Loop
Escherichia coli	FtsN	1UTA	252–312	Loop	Loop
Escherichia coli	OmpA	2MQE	290–302	Loop	α-Helix
Escherichia coli	RcsF	2Y1B	74–118[c]	β-Sheet	β-Sheet
			109–124[c]	β-Sheet	β-Sheet
Escherichia coli	ZnuA	2OGW	252–306	Loop	α-Helix
Escherichia coli	LivK	1USG	53–78	Loop	Loop
Escherichia coli	Bla	3JYI	77–123	α-Helix	α-Helix
Escherichia coli	Pbp4	2EX9	168–178	α-Helix	Loop
			217–234	Loop	β-Sheet
Escherichia coli	PhoA	1ALK	169–179	Loop	Loop
			286–336	Loop	α-Helix
Escherichia coli	DppA	1DPE	6–234	β-Sheet	Loop
			422–435	Loop	Loop
Klebsiella oxytoca	PulS	4A56	53–107	Loop	α-Helix
Pseudomonas aeruginosa	LasB	1EZM	30–58	Loop	Loop
			270–297	α-Helix	Loop
Pseudomonas aeruginosa	PilA	1OQW	129–142	β-Sheet	Loop
Pseudomonas aeruginosa	LipA	1EX9	183–235	Loop	Loop
Shigella flexneri	LptD	4Q35	31–724[c]	α-Helix	Loop
			173–725[c]	Loop	Loop
Vibrio cholerae	CtxB	1CHP	9–86	α-Helix	β-Sheet
Vibrio cholerae	TcpA	1OQV	120–186	α-Helix	Loop
Yersinia pestis	Caf1M	1P5U	101–140	β-Sheet	β-Sheet

[a] Amino acid position of cysteines that form a disulfide bond in the mature form of each substrate.
[b] Secondary structure location of cysteines that form disulfide bonds.
[c] Substrates with non-consecutive disulfide bonds and therefore would require a combined action of DsbA and DsbC.

To date, the exquisite diversity of the DsbA substrates has not been comprehensively analyzed. Although it is accepted that DsbA enzymes catalyze disulfide bond formation in unfolded proteins as they are transported through the cytoplasmic membrane [68], we sought to understand what types of secondary and tertiary structures require disulfide bonds for stability and are folded by DsbA. With the knowledge that not all cysteine residues participate in disulfide bonds, this observation could allow for a better prediction of which proteins and local structures acquire disulfide bonds. To gain a better understanding of the structural class of substrate proteins folded by DsbA, a protein dataset was constructed containing 43 pathogenicity associated substrates that have been previously functionally characterized (Table S1) [4,5,20]. Among these 43 substrates, 28 have three-dimensional structures available in the Protein Data Bank (PDB) (Table 2). These 28 substrates with known structures, were then classified with the CATH-Gene3D Protein Structure Classification Database v4.2 [76,77] at: (i) class level according to their secondary structure content; (ii) architecture level according to the secondary structure arrangement in three-dimensional space independent of connectivity; (iii) topology/fold level according to their topological connections and number of secondary structures [76,78].

The 28 DsbA substrates, which collectively encompass 32 protein domains harboring disulfide bonds (S2 subunit, DppA, LptD and LasB substrates, each have two domains with disulfides, (Table 2)), were found to be organized into three different classes according to the secondary structure content, with slightly more than half having a αβ-structures (59%), followed by mainly β-sheets (31%) and mainly α-helix (10%) (Fig. 6, Table S1). At the architecture level, 11 different architectures were identified, with ~56% showing a sandwich type architecture (22% 2-layer sandwich, 19% 3-layer (αβα) sandwich, 12% sandwich and 3% 3-layer (ββα) sandwich) (Fig. 6). Finally, this analysis found 25 different folds at the topology level, with the immunoglobulin (Ig-), Rossman and oligonucleotide/oligosaccharide binding (OB-) folds being the most prominent type among the structurally characterized DsbA substrates.

The Ig-fold is widely distributed in nature, present in vertebrates, invertebrates, plants, fungi, parasites, bacteria and viruses [79]. This fold is characterized by a pair of β-sheets often linked by a disulfide bond and composed of antiparallel β-strands surrounding a central hydrophobic core [80] (Fig. 7B, Caf1M). The wide occurrence of the Ig-fold has been attributed to its functional plasticity and its specific structural characteristics that confer stability and resistance to proteolysis [80]. Our structural classification of DsbA substrates revealed that proteins with an Ig-fold include the periplasmic fimbrial chaperones PapD from *E. coli*, one of the first examples of Ig-fold proteins identified in bacteria
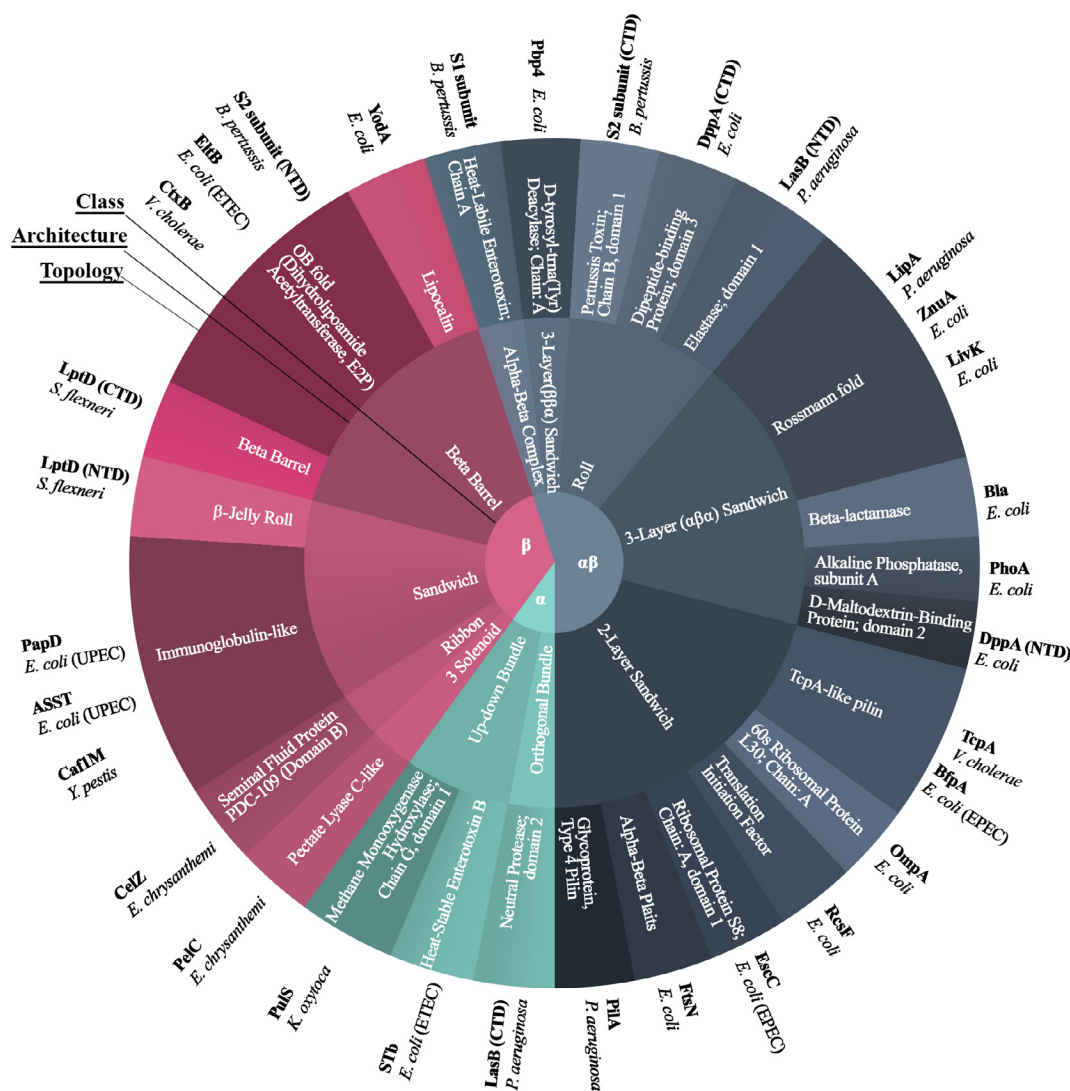
Fig. 6. CATH classification of disulfide bond containing domains from structurally characterised DsbA substrates. Classification of DsbA substrates by class according to: Secondary structure content (inner circle), substrates divided into mainly α-helices (α) (cyan), mainly β-sheets (β) (raspberry) and a combination of both (αβ) (deep teal); Architecture (middle circle), substrates divided into 11 different architectures; and Topology (outer circle), DsbA substrates display 25 different folds at the topology level. EPEC: Enteropathogenic *E. coli*; ETEC: Enterotoxigenic *E. coli*; UPEC: Uropathogenic *E. coli*; NTC: N-terminal domain; CTD: C-terminal domain. (For interpretation of the references to colour in this figure legend, the reader is referred to the web version of this article.)

[81,82], and Caf1M from *Y. pestis* [83] involved in the process of adhesion [84]; and ASST from *E. coli* [63] involved in the detoxification of phenolic compounds.

The OB-fold (Fig. 7B, CtxB) varies from between 70 and 150 amino acids in length and is characterized by 5 highly coiled antiparallel β-sheets arranged into β barrels, with an α-helix capped at one end and a binding cleft at the other. Proteins showcasing this type of fold have the ability to establish protein-DNA, -RNA or -protein interactions and so are usually involved in a number of cellular processes such as DNA replication and repair, and activation of the DNA-damage checkpoint pathways [85–87]. DsbA substrates found to have this type of fold include secreted toxins such as CtxB from *V. cholerae* [87–89], EltB from *E. coli* [87,90], and the N-terminal domain of S2 subunit from *B. pertussis* [91,92].

The Rossmann fold (Fig. 6, LipA) is one of the most common folds found in proteins of the αβ class [93]. This fold is characterized by a conserved (βαβ) motif that works as a place of contact with the ADP portion of dinucleotides, namely, FAD, NAD and NADP. The overall Rossmann fold is composed of a single parallel β-sheet constituted by two sets of β-α-β-α-β units that forms a

3-layer (α/β/α) sandwich [93–95] (Fig. 7C). DsbA substrates found to have this fold include LivK [96,97] and ZnuA [98] from *E. coli* involved in the process of amino acid and metal transport (zinc) respectively; and LipA [99] from *P. aeruginosa* involved in biofilm formation.

Overall, although our substrate database only captures a very small fraction of the DsbA interactome, this analysis clearly showcases the large array of structurally diverse substrates folded by DsbA and highlights how DsbA proteins indiscriminately introduce disulfide bonds in a plethora of proteins leading to different types of protein folds.

5.1. Common features of DsbA substrates

Although DsbA introduces disulfide bonds to unfolded substrates, we wondered what structural elements harbor DsbA mediated disulfides. Using PDBsum [118] in combination with PyMol we analyzed the three-dimensional structures of the 28 characterized substrates (Table 2), to identify the secondary structures that contain disulfide bond forming cysteine residues. In particular, we
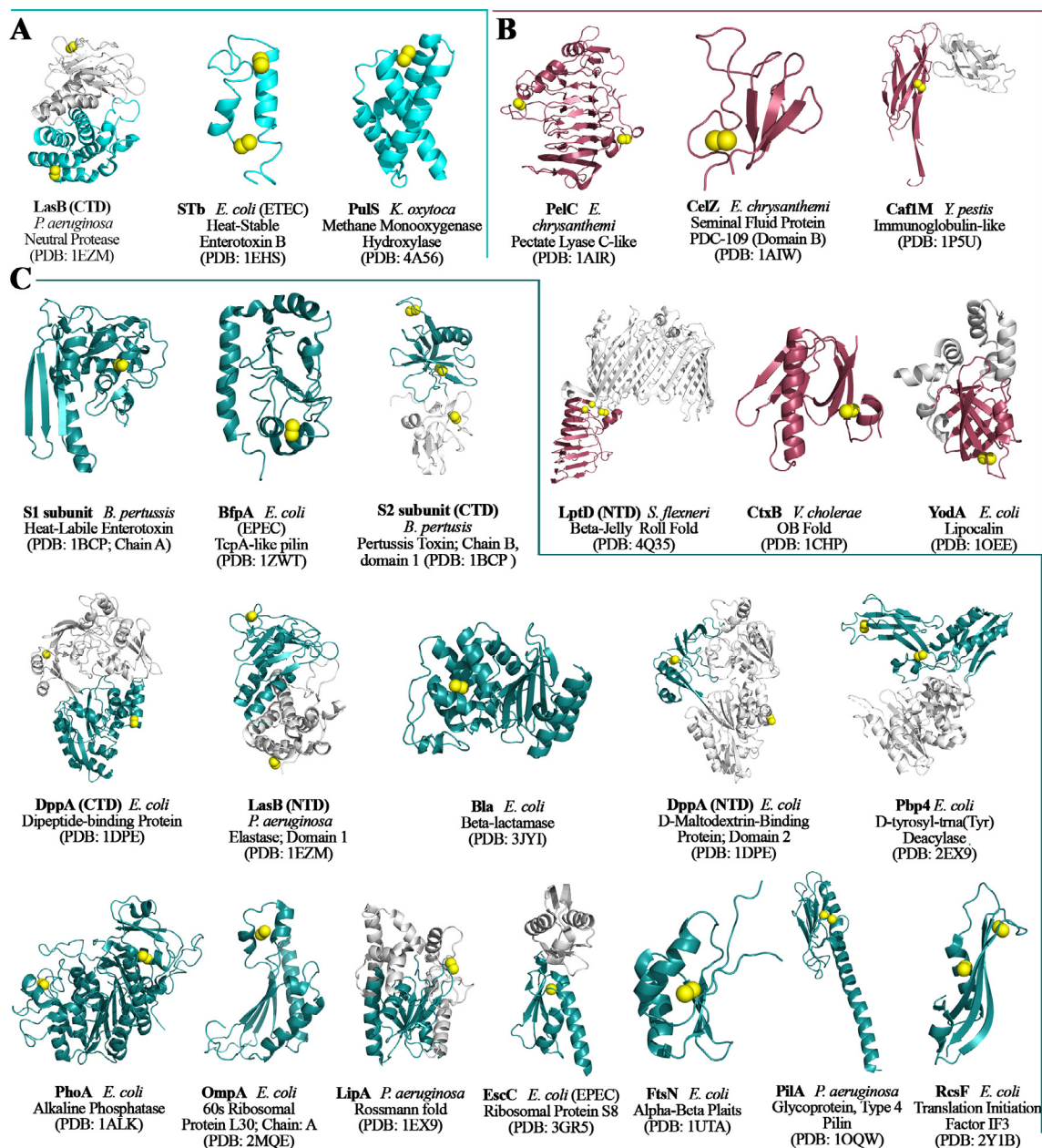
Fig. 7. Examples of DsbA substrates with different folds grouped by class. A. Cartoon representation of mainly α-helix class for substrates LasB (CTD) [100], STb [101] and PulS [102]. Fold is highlighted in cyan, sulfur atoms from disulfide bonds shown as yellow spheres and the rest of the protein shown in white. B. Cartoon representation of mainly β-sheets class for substrates PelC [103], CelZ [104], Caf1M [105], CtxB [88] and YodA [106]. Folds are highlighted in raspberry, sulfur atoms from disulfide bonds shown as yellow spheres and the rest of the protein shown in white. C. Cartoon representation of αβ class for substrates S1 subunit [92], RcsF [107], Pbp4 [108], S2 subunit (CTD) [92], DppA (CTD) [109], LasB (NTD) [110], LipA [99], Bla [111], DppA (NTD) [109], BpfA [112], PhoA [113], OmpA [114], EscC [115], FtsN [116], LptD (NTD)[100] and PilA [117]. Folds are highlighted in deep teal, sulfur atoms from disulfide bonds shown as yellow spheres and the rest of the protein shown in white. For each structure, substrate name, organism of origin, fold and PDB codes are provided. NTD: N-terminal domain; CTD: C-terminal domain. (For interpretation of the references to colour in this figure legend, the reader is referred to the web version of this article.)

focused on substrates with a single disulfide or consecutive disulfides, which would be directly formed by DsbA (three substrates, *E. coli* STb, RcsF and LptD, each have two non-consecutive disulfide bonds and therefore would require the combined action of DsbA and DsbC). From this analysis, it was found that disulfide bonds are formed between cysteine residues irrespective of their position in their primary sequence (Table 2). Additionally, for 80.6% of the total number of disulfide bonds found within these substrates, at least one of the cysteines that forms a disulfide bond is harbored within a loop, with the remaining 19.4% found either in an α-helix or a β-sheet (Table 2) (Fig. 7). The presence of disulfide bonds

in loops may ensure the local stability of these structural elements that frequently harbor active site residues required for function [119,120 121–123].

DsbA is thought to recognize the most N-terminal cysteine in each disulfide bond forming cysteine pair, when proteins are delivered unfolded via the Sec system frequently in an N- to C-terminal direction [6,68]. In order to investigate if there is a DsbA recognition motif, we specifically focused on *Ec*DsbA substrates, as this class Ia DsbA comprises the largest collection of structurally characterised substrates for which we know the disulfide connectivity (Table 2). For each one of these substrates, the first cysteine
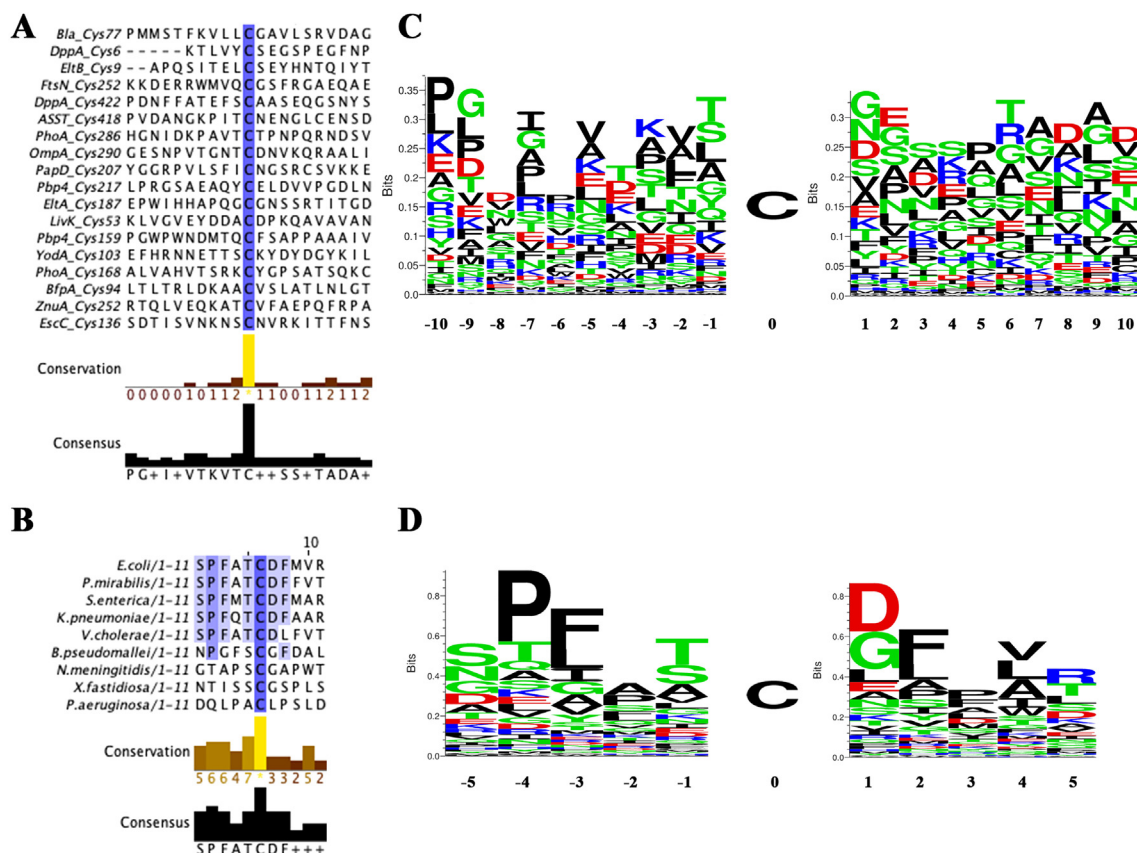
Fig. 8. Enrichment of amino acids around cysteine residues of *E. coli* DsbA substrates and class I DsbA oxidases. A. Multiple sequence alignment of 10 amino acids preceding and succeeding cysteine residues of substrates involved in interaction with *Ec*DsbA. B. Multiple sequence alignment of 5 amino acid residues preceding and succeeding the cysteine residues of DsbB involved in interaction with Class I DsbAs. For panels A and B sequences were colored from most conserved (dark blue) to less conserved (light blue). Conservation and consensus histograms are shown below each alignment. C. Position-specific enrichment of 10 amino acids preceding and succeeding the substrate cysteine residues involved in interaction with *Ec*DsbA. D. Position-specific enrichment of 5 amino acids preceding and succeeding the DsbB cysteine residues involved in interaction with Class I DsbAs. For panels C and D, cysteine residues are shown at position 0 with preceding and succeeding amino acids shown as a Shannon logo type. The stack of symbols at each position represents amino acids, with frequently observed amino acids shown as large symbols. Conserved and variable positions are represented as big and small stacks respectively. Acidic amino acids (DE) are shown in red, neutral amino acids (QSTYNG) are shown in green, basic amino acids (HKR) are shown in blue and aliphatic amino acids (IALVPFM) are shown in black. (For interpretation of the references to colour in this figure legend, the reader is referred to the web version of this article.)

involved in the formation of a disulfide bond together with its flanking 10 amino acids were extracted for analysis. These sequences were then aligned using the software Jalview (V 2.10.5) (Fig. 8A). Additionally, the Shannon sequence logo generated with the online server Seq2Logo [124] was used to visualize the frequency of amino acids preceding and succeeding the cysteine residues (Fig. 8C). No significant amino acid conservation was observed among *Ec*DsbA substrates, although a predominance of small-medium uncharged amino acids were enriched surrounding the substrate target cysteines. The diversity of DsbA substrates made the identification of a consensus motif challenging, however this analysis informed about the chemical properties that underline *Ec*DsbA-substrate interactions, which may be beneficial for the development of inhibitors targeting the DsbA substrate recognition site. It is important to note that this analysis may not be applicable to substrates of other DsbA proteins, particularly those interacting with DsbAs from classes other than Ia [39].

For comparison, we also analyzed the recognition site surrounding the DsbB cysteine known to interact with DsbA (first cysteine residue in the second periplasmic loop). For this analysis, we selected DsbB proteins from nine organisms containing class I DsbAs, since previous work has shown that these DsbBs interact with DsbA proteins in a similar mode (Fig. 3). The amino acid sequences surrounding the DsbB cysteine residue directly interact-

ing with DsbA were retrieved from Uniprot (Table S2). An alignment of these sequences was performed using Jalview (Fig. 8B) followed by a position specific amino acid enrichment analysis using Seq2Logo (Fig. 8D) [124]. These analyses revealed a somewhat more conserved consensus sequence surrounding the cysteine residue consisting of S(56%)–P(67%)–F(56%)–A(33%)–T(56%)–C(100%)–D(56%)–F(56%). Although DsbB homologues are expected to share higher sequence homology than a diverse set of substrates, this finding reflects the somewhat different binding mode of the cognate oxidases compared to protein substrates, whereby the presence of aromatic residues neighboring the DsbB cysteine would facilitate the interaction with the hydrophobic groove [27] characteristic of class I DsbA proteins [39].

6. Summary and outlook

As the threat of antibiotic resistance continues to grow, it has become increasingly important to understand the molecular mechanism of bacterial pathogenesis. The reliance of virulence factors on DSB systems for their assembly, has indisputably linked these proteins, primarily DsbA thiol oxidases to the bacterial pathogenic potential. This, in addition to the wide distribution of DSBs across bacteria, make these systems attractive targets to disrupt bacterial

pathogenesis. In this review we have summarized the current knowledge on DsbA proteins including their structural diversity as well as their biochemical and functional properties. We have particularly focused on the DsbA interactome; collating the current understanding of how this enzyme interacts with cognate DsbB oxidases and explored the sequence and structural diversity of DsbA substrates. This detailed examination, has allowed us to identify that cysteine residues interacting with DsbA are primarily present in loop regions of both substrates and cognate oxidases. Furthermore, we have proposed a consensus motif recognized by class I DsbA proteins in DsbB oxidases. Overall, a detailed understanding of how these important redox enzymes interact with partner proteins, not only provides fundamental understanding on the bacterial oxidative protein folding machinery but may offer tools to allow the identification of so far unexplored DsbA substrates.

As DsbA plays a pivotal role in bacterial virulence, inhibitors of DsbA are being actively pursued as anti-microbial agents [125]. There are a number of advantages to targeting these redox enzymes; firstly, in conditions where DsbAs are not essential for viability or growth, their inhibition would reduce virulence and likely impose low selection pressure for resistance development [126]. Secondly, DsbA is present in the periplasm, which is more accessible relative to cytoplasmic targets. Furthermore, all DsbA inhibitors described so far target the hydrophobic groove of DsbA [47,66,125,127–130], which is not present in human thioredoxin or PDI. Therefore, despite DsbA belonging to the widespread thioredoxin superfamily, DsbA-tailored inhibitors are less likely to inhibit TRX-like proteins in humans. The detailed analysis of the DsbA-substrate and DsbA-DsbB interactions described in this work could therefore inform a number of international campaigns in their efforts to designing specific inhibitors against DsbA enzymes [47,66,125,127–130].

CRediT authorship contribution statement

Carlos Santos-Martin: Conceptualization, Writing – original draft, Data curation, Formal analysis. **Geqing Wang:** Conceptualization, Writing – original draft, Data curation, Formal analysis. **Pramod Subedi:** Writing – original draft. **Lilian Hor:** Writing – review & editing. **Makrina Totsika:** Writing – review & editing. **Jason John Paxman:** Formal analysis, Writing – review & editing. **Begoña Heras:** Conceptualization, Funding acquisition, Writing – review & editing.

Declaration of Competing Interest

The authors declare that they have no known competing financial interests or personal relationships that could have appeared to influence the work reported in this paper.

Acknowledgements

Appendix A. Supplementary data

Supplementary data to this article can be found online at https://doi.org/10.1016/j.csbj.2021.08.018.

References

[1] Beceiro A, Tomás M, Bou G. Antimicrobial Resistance and Virulence: a Successful or Deleterious Association in the Bacterial World? Clin Microbiol Rev 2013;26(2):185.

[2] Diard M, Hardt WD. Evolution of bacterial virulence. FEMS Microbiol Rev 2017;41(5):679–97.

[3] Sharma AK, Dhasmana N, Dubey N, Kumar N, Gangwal A, Gupta M, et al. Bacterial Virulence Factors: Secreted for Survival. Indian J Microbiol 2017;57(1):1–10.

[4] Heras B et al. DSB proteins and bacterial pathogenicity. Nat Rev Microbiol 2009;7:215.

[5] Landeta C, Boyd D, Beckwith J. Disulfide bond formation in prokaryotes. Nat Microbiol 2018;3(3):270–80.

[6] Bardwell JCA, McGovern K, Beckwith J. Identification of a protein required for disulfide bond formation in vivo. Cell 1991;67(3):581–9.

[7] Akiyama Y, Kamitani S, Kusukawa N, Ito K. In vitro catalysis of oxidative folding of disulfide-bonded proteins by the Escherichia coli dsbA (ppfA) gene product. J Biol Chem 1992;267(31):22440–5.

[8] Bringer M-A, Rolhion N, Glasser A-L, Darfeuille-Michaud A. The oxidoreductase DsbA plays a key role in the ability of the Crohn's disease-associated adherent-invasive Escherichia coli strain LF82 to resist macrophage killing. J Bacteriol 2007;189(13):4860–71.

[9] Burall LS, Harro JM, Li X, Lockatell CV, Himpsl SD, Hebel JR, et al. Proteus mirabilis genes that contribute to pathogenesis of urinary tract infection: identification of 25 signature-tagged mutants attenuated at least 100-fold. Infect Immun 2004;72(5):2922–38.

[10] Coulthurst SJ, Lilley KS, Hedley PE, Liu H, Toth IK, Salmond GPC. DsbA plays a critical and multifaceted role in the production of secreted virulence factors by the phytopathogen Erwinia carotovora subsp. atroseptica. J Biol Chem 2008;283(35):23739–53.

[11] Lee SH, Butler SM, Camilli A. Selection for in vivo regulators of bacterial virulence. Proc Natl Acad Sci U S A 2001;98(12):6889–94.

[12] Lin D, Rao CV, Slauch JM. The Salmonella SPI1 type three secretion system responds to periplasmic disulfide bond status via the flagellar apparatus and the RcsCDB system. J Bacteriol 2008;190(1):87–97.

[13] Meima R, Eschevins C, Fillinger S, Bolhuis A, Hamoen LW, Dorenbos R, et al. The bdbDC operon of Bacillus subtilis encodes thiol-disulfide oxidoreductases required for competence development. J Biol Chem 2002;277(9):6994–7001.

[14] Peek JA, Taylor RK. Characterization of a periplasmic thiol:disulfide interchange protein required for the functional maturation of secreted virulence factors of Vibrio cholerae. Proc Natl Acad Sci U S A 1992;89(13):6210–4.

[15] Tomb JF. A periplasmic protein disulfide oxidoreductase is required for transformation of Haemophilus influenzae Rd. Proc Natl Acad Sci U S A 1992;89(21):10252–6.

[16] Yu J. Inactivation of DsbA, but not DsbC and DsbD, affects the intracellular survival and virulence of Shigella flexneri. Infect Immun 1998;66(8):3909–17.

[17] Ireland PM, McMahon RM, Marshall LE, Halili M, Furlong E, Tay S, et al. Disarming Burkholderia pseudomallei: structural and functional characterization of a disulfide oxidoreductase (DsbA) required for virulence in vivo. Antioxid Redox Signal 2014;20(4):606–17.

[18] Basharov MA. Protein folding. J Cell Mol Med 2003;7(3):223–37.

[19] Totsika M, Heras Begon~a, Wurpel DJ, Schembri MA. Characterization of two homologous disulfide bond systems involved in virulence factor biogenesis in uropathogenic Escherichia coli CFT073. J Bacteriol 2009;191(12):3901–8.

[20] Shouldice SR, Heras B, Walden PM, Totsika M, Schembri MA, Martin JL. Structure and function of DsbA, a key bacterial oxidative folding catalyst. Antioxid Redox Signal 2011;14(9):1729–60.

[21] Sevier CS, Kaiser CA. Formation and transfer of disulphide bonds in living cells. Nat Rev Mol Cell Biol 2002;3(11):836–47.

[22] Wiedemann C et al. Cysteines and Disulfide Bonds as Structure-Forming Units: Insights From Different Domains of Life and the Potential for Characterization by NMR. Front Chem 2020;8(280).

[23] Hiniker A, Bardwell JCA. In vivo substrate specificity of periplasmic disulfide oxidoreductases. J Biol Chem 2004;279(13):12967–73.

[24] Zapun A, Missiakas D, Raina S, Creighton TE. Structural and Functional Characterization of DsbC, a Protein Involved in Disulfide Bond Formation in Escherichia coli. Biochem 1995;34(15):5075–89.

[25] Missiakas D, Georgopoulos C, Raina S. The Escherichia coli dsbC (xprA) gene encodes a periplasmic protein involved in disulfide bond formation. EMBO J 1994;13(8):2013–20.

[26] Bardwell JC, Lee JO, Jander G, Martin N, Belin D, Beckwith J. A pathway for disulfide bond formation in vivo. Proc Natl Acad Sci U S A 1993;90(3):1038–42.

[27] Inaba K, Murakami S, Suzuki M, Nakagawa A, Yamashita E, Okada K, et al. Crystal structure of the DsbB-DsbA complex reveals a mechanism of disulfide bond generation. Cell 2006;127(4):789–801.

[28] Missiakas D, Georgopoulos C, Raina S. Identification and characterization of the Escherichia coli gene dsbB, whose product is involved in the formation of disulfide bonds in vivo. Proc Natl Acad Sci U S A 1993;90(15):7084–8.

[29] Rietsch A, Bessette P, Georgiou G, Beckwith J. Reduction of the periplasmic disulfide bond isomerase, DsbC, occurs by passage of electrons from cytoplasmic thioredoxin. J Bacteriol 1997;179(21):6602–8.

[30] Martin JL, Bardwell JCA, Kuriyan J. Crystal structure of the DsbA protein required for disulphide bond formation in vivo. Nature 1993;365 (6445):464–8.

[31] Grauschopf U et al. Why is DsbA such an oxidizing disulfide catalyst? Cell 1995;83(6):947–55.

[32] Guddat LW, Bardwell JCA, Martin JL. Crystal structures of reduced and oxidized DsbA: investigation of domain motion and thiolate stabilization. Structure 1998;6(6):757–67.

[33] Charbonnier J-B, Belin P, Moutiez M, Stura EA, Quéméneur E. On the role of the cis-proline residue in the active site of DsbA. Protein Sci 1999;8 (1):96–105.

[34] Ren G, Stephan D, Xu Z, Zheng Y, Tang D, Harrison RS, et al. Properties of the thioredoxin fold superfamily are modulated by a single amino acid residue. J Biol Chem 2009;284(15):10150–9.

[35] Guddat LW, Martin JL, Bardwell JCA, Zander T. The uncharged surface features surrounding the active site of Escherichia coli DsbA are conserved and are implicated in peptide binding. Protein Sci 1997;6(6):1148–56.

[36] Paxman JJ, Borg NA, Horne J, Thompson PE, Chin Y, Sharma P, et al. The structure of the bacterial oxidoreductase enzyme DsbA in complex with a peptide reveals a basis for substrate specificity in the catalytic cycle of DsbA enzymes. J Biol Chem 2009;284(26):17835–45.

[37] Darby NJ, Creighton TE. Catalytic mechanism of DsbA and its comparison with that of protein disulfide isomerase. Biochem 1995;34(11):3576–87.

[38] Skórko-Glonek J, Sobiecka-Szkatuła A, Lipińska B. Characterization of disulfide exchange between DsbA and HtrA proteins from Escherichia coli. Acta Biochim Pol 2006;53(3):585–9.

[39] McMahon RM, Premkumar L, Martin JL. Four structural subclasses of the antivirulence drug target disulfide oxidoreductase DsbA provide a platform for design of subclass-specific inhibitors. Biochim Biophys Acta 2014;1844 (8):1391–401.

[40] Kurth F, Duprez W, Premkumar L, Schembri MA, Fairlie DP, Martin JL. Crystal structure of the dithiol oxidase DsbA enzyme from proteus mirabilis bound non-covalently to an active site peptide ligand. J Biol Chem 2014;289 (28):19810–22.

[41] Heras B, Totsika M, Jarrott R, Shouldice SR, Gunčar G, Achard MES, et al. Structural and functional characterization of three DsbA paralogues from Salmonella enterica serovar typhimurium. J Biol Chem 2010;285 (24):18423–32.

[42] Bouwman CW, Kohli M, Killoran A, Touchie GA, Kadner RJ, Martin NL. Characterization of SrgA, a Salmonella enterica serovar Typhimurium virulence plasmid-encoded paralogue of the disulfide oxidoreductase DsbA, essential for biogenesis of plasmid-encoded fimbriae. J Bacteriol 2003;185 (3):991–1000.

[43] Walden PM et al. The 1.2 Å resolution crystal structure of TcpG, the Vibrio cholerae DsbA disulfide-forming protein required for pilus and cholera-toxin production. Acta Crystallogr Sect C Cryst Struct Commun 2012;68(Pt 10):1290–302.

[44] Kurth F et al. Comparative sequence, structure and redox analyses of Klebsiella pneumoniae DsbA show that anti-virulence target DsbA enzymes fall into distinct classes. PLoS ONE 2013;8(11):e80210.

[45] Shouldice SR, Heras B, Jarrott R, Sharma P, Scanlon MJ, Martin JL. Characterization of the DsbA oxidative folding catalyst from Pseudomonas aeruginosa reveals a highly oxidizing protein that binds small molecules. Antioxid Redox Signal 2010;12(8):921–31.

[46] Heras B, Kurz M, Jarrott R, Shouldice SR, Frei P, Robin G, et al. Staphylococcus aureus DsbA does not have a destabilizing disulfide. A new paradigm for bacterial oxidative folding. J Biol Chem 2008;283(7):4261–71.

[47] Totsika M, Vagenas D, Paxman JJ, Wang G, Dhouib R, Sharma P, et al. Inhibition of Diverse DsbA Enzymes in Multi-DsbA Encoding Pathogens. Antioxid Redox Signal 2018;29(7):653–66.

[48] Lafaye C, Iwema T, Carpentier P, Jullian-Binard C, Kroll JS, Collet J-F, et al. Biochemical and structural study of the homologues of the thiol-disulfide oxidoreductase DsbA in Neisseria meningitidis. J Mol Biol 2009;392 (4):952–66.

[49] Kurz M et al. Structural and functional characterization of the oxidoreductase alpha-DsbA1 from Wolbachia pipientis. Antioxid Redox Signal 2009;11 (7):1485–500.

[50] Huber-Wunderlich M, Glockshuber R. A single dipeptide sequence modulates the redox properties of a whole enzyme family. Fold Des 1998;3(3):161–71.

[51] Hu S-H, Peek JA, Rattigan E, Taylor RK, Martin JL. Structure of TcpG, the DsbA protein folding catalyst from Vibrio cholerae11Edited by I. A. Wilson. J Mol Biol 1997;268(1):137–46.

[52] Dumoulin A, Grauschopf U, Bischoff M, Thöny-Meyer L, Berger-Bächi B. Staphylococcus aureus DsbA is a membrane-bound lipoprotein with thiol-disulfide oxidoreductase activity. Arch Microbiol 2005;184(2):117–28.

[53] Rinaldi FC, Meza AN, Guimarães BG. Structural and Biochemical Characterization of Xylella fastidiosa DsbA Family Members: New Insights into the Enzyme−Substrate Interaction. Biochemistry 2009;48(15):3508–18.

[54] Grimshaw JPA, Stirnimann CU, Brozzo MS, Malojcic G, Grütter MG, Capitani G, et al. DsbL and DsbI form a specific dithiol oxidase system for periplasmic arylsulfate sulfotransferase in uropathogenic Escherichia coli. J Mol Biol 2008;380(4):667–80.

[55] Vivian JP, Scoullar J, Rimmer K, Bushell SR, Beddoe T, Wilce MCJ, et al. Structure and function of the oxidoreductase DsbA1 from Neisseria meningitidis. J Mol Biol 2009;394(5):931–43.

[56] Crow A, Lewin A, Hecht O, Carlsson Möller M, Moore GR, Hederstedt L, et al. Crystal structure and biophysical properties of Bacillus subtilis BdbD. An oxidizing thiol:disulfide oxidoreductase containing a novel metal site. J Biol Chem 2009;284(35):23719–33.

[57] Subedi P et al. Salmonella enterica BcfH Is a Trimeric Thioredoxin-Like Bifunctional Enzyme with Both Thiol Oxidase and Disulfide Isomerase Activities. Antioxid Redox Signal 2021;35(1):21–39.

[58] Dutton RJ, Boyd D, Berkmen M, Beckwith J. Bacterial species exhibit diversity in their mechanisms and capacity for protein disulfide bond formation. Proc Natl Acad Sci U S A 2008;105(33):11933–8.

[59] Guo K et al. Complex Oxidation of Apocytochromes c during Bacterial Cytochrome c Maturation. Appl Environ Microbiol 2019;85(24).

[60] Gupta SD, Wu HC, Rick PD. A Salmonella typhimurium genetic locus which confers copper tolerance on copper-sensitive mutants of Escherichia coli. J Bacteriol 1997;179(16):4977–84.

[61] Shepherd M, Heras B, Achard MES, King GJ, Argente MP, Kurth F, et al. Structural and functional characterization of ScsC, a periplasmic thioredoxin-like protein from Salmonella enterica serovar Typhimurium. Antioxid Redox Signal 2013;19(13):1494–506.

[62] Subedi P, Paxman JJ, Wang G, Ukuwela AA, Xiao Z, Heras B. The Scs disulfide reductase system cooperates with the metallochaperone CueP in Salmonella copper resistance. J Biol Chem 2019;294(44):15876–88.

[63] Malojčić G, Owen RL, Glockshuber R. Structural and Mechanistic Insights into the PAPS-Independent Sulfotransfer Catalyzed by Bacterial Aryl Sulfotransferase and the Role of the DsbL/DsbI System in Its Folding. Biochemistry 2014;53(11):1870–7.

[64] Inaba K, Murakami S, Nakagawa A, Iida H, Kinjo M, Ito K, et al. Dynamic nature of disulphide bond formation catalysts revealed by crystal structures of DsbB. EMBO J 2009;28(6):779–91.

[65] Guddat LW, Bardwell JCA, Glockshuber R, Huber-Wunderlich M, Zander T, Martin JL. Structural analysis of three His32 mutants of DsbA: support for an electrostatic role of His32 in DsbA stability. Protein Sci 1997;6(9):1893–900.

[66] Duprez W, Premkumar L, Halili MA, Lindahl F, Reid RC, Fairlie DP, et al. Peptide Inhibitors of the Escherichia coli DsbA Oxidative Machinery Essential for Bacterial Virulence. J Med Chem 2015;58(2):577–87.

[67] McMahon RM et al. Virulence of the Melioidosis Pathogen Burkholderia pseudomallei Requires the Oxidoreductase Membrane Protein DsbB. Infect Immun 2018;86(5).

[68] Kadokura H, Beckwith J. Detecting folding intermediates of a protein as it passes through the bacterial translocation channel. Cell 2009;138 (6):1164–73.

[69] Fernandes PA, Ramos MJ. Theoretical insights into the mechanism for thiol/disulfide exchange. Chemistry 2004;10(1):257–66.

[70] Frech C, Wunderlich M, Glockshuber R, Schmid FX. Preferential binding of an unfolded protein to DsbA. EMBO J 1996;15(2):392–8.

[71] Couprie J, Vinci F, Dugave C, Quéméneur E, Moutiez M. Investigation of the DsbA Mechanism through the Synthesis and Analysis of an Irreversible Enzyme−Ligand Complex. Biochemistry 2000;39(22):6732–42.

[72] Premkumar L, Kurth F, Duprez W, Grøftehauge MK, King GJ, Halili MA, et al. Structure of the Acinetobacter baumannii Dithiol Oxidase DsbA Bound to Elongation Factor EF-Tu Reveals a Novel Protein Interaction Site. J Biol Chem 2014;289(29):19869–80.

[73] Collet J-F, Messens J. Structure, function, and mechanism of thioredoxin proteins. Antioxid Redox Signal 2010;13(8):1205–16.

[74] Kadokura H et al. Snapshots of DsbA in action: detection of proteins in the process of oxidative folding. Science 2004;303(5657):534–7.

[75] Fujimoto T, Inaba K, Kadokura H. Methods to identify the substrates of thiol-disulfide oxidoreductases. Protein Sci 2019;28(1):30–40.

[76] Dawson NL et al. CATH: an expanded resource to predict protein function through structure and sequence. Nucleic Acids Res 2016;45(D1):D289–95.

[77] Lewis TE et al. Gene3D: Extensive prediction of globular domains in proteins. Nucleic Acids Res 2017;46(D1):D435–9.

[78] Greene LH et al. The CATH domain structure database: new protocols and classification levels give a more comprehensive resource for exploring evolution. Nucleic Acids Res 2007;35(Database issue):D291–7.

[79] Halaby DM, Mornon JPE. The immunoglobulin superfamily: An insight on its tissular, species, and functional diversity. J Mol Evol 1998;46(4):389–400.

[80] Bodelón G, Palomino C, Fernández LÁ. Immunoglobulin domains in Escherichia coli and other enterobacteria: from pathogenesis to applications in antibody technologies. FEMS Microbiol Rev 2013;37 (2):204–50.

[81] Waksman G, Hultgren SJ. Structural biology of the chaperone-usher pathway of pilus biogenesis. Nat Rev Microbiol 2009;7(11):765–74.

[82] Holmgren A, Bränden C-L. Crystal structure of chaperone protein PapD reveals an immunoglobulin fold. Nature 1989;342(6247):248–51.

[83] Zavialov AV, Knight SD. A novel self-capping mechanism controls aggregation of periplasmic chaperone Caf1M. Mol Microbiol 2007;64(1):153–64.

[84] Vincent-Sealy LV et al. Erwinia carotovora DsbA mutants: evidence for a periplasmic-stress signal transduction system affecting transcription of genes encoding secreted proteins. Microbiology 1999;145(Pt 8):1945–58.

[85] Flynn RL, Zou L. Oligonucleotide/oligosaccharide-binding fold proteins: a growing family of genome guardians. Crit Rev Biochem Mol Biol 2010;45 (4):266–75.

[86] Arcus V. OB-fold domains: a snapshot of the evolution of sequence, structure and function. Curr Opin Struct Biol 2002;12(6):794–801.

[87] Murzin AG. OB(oligonucleotide/oligosaccharide binding)-fold: common structural and functional solution for non-homologous sequences. EMBO J 1993;12(3):861–7.

[88] Merritt EA, Sarfaty S, Chang T-T, Palmer LM, Jobling MG, Holmes RK, et al. Surprising leads for a cholera toxin receptor-binding antagonist: crystallographic studies of CTB mutants. Structure 1995;3(6):561–70.

[89] Aman AT, Fraser S, Merritt EA, Rodigherio C, Kenny M, Ahn M, et al. A mutant cholera toxin B subunit that binds GM1- ganglioside but lacks immunomodulatory or toxic activity. Proc Natl Acad Sci U S A 2001;98(15):8536–41.

[90] Matković-Calogović D, Loregian A, D'Acunto MR, Battistutta R, Tossi A, Palù G, et al. Crystal structure of the B subunit of Escherichia coli heat-labile enterotoxin carrying peptides with anti-herpes simplex virus type 1 activity. J Biol Chem 1999;274(13):8764–9.

[91] Millen SH et al. Single Amino Acid Polymorphisms of Pertussis Toxin Subunit S2 (PtxB) Affect Protein Function. PLoS ONE 2015;10(9):e0137379.

[92] Hazes B, Boodhoo A, Cockle SA, Read RJ. Crystal structure of the pertussis toxin-ATP complex: a molecular sensor. J Mol Biol 1996;258(4):661–71.

[93] Medvedev KE, Kinch LN, Grishin NV. Functional and evolutionary analysis of viral proteins containing a Rossmann-like fold. Protein Sci 2018;27(8):1450–63.

[94] Hanukoglu I. Proteopedia: Rossmann fold: A beta-alpha-beta fold at dinucleotide binding sites. Biochem Mol Biol Educ 2015;43(3):206–9.

[95] Rossmann MG, Moras D, Olsen KW. Chemical and biological evolution of a nucleotide-binding protein. Nature 1974;250(5463):194–9.

[96] Magnusson U, Salopek-Sondi B, Luck LA, Mowbray SL. X-ray structures of the leucine-binding protein illustrate conformational changes and the basis of ligand specificity. J Biol Chem 2004;279(10):8747–52.

[97] Sack JS et al. Structure of the L-leucine-binding protein refined at 2.4 A resolution and comparison with the Leu/Ile/Val-binding protein structure. J Mol Biol 1989;206(1):193–207.

[98] Chandra BR, Yogavel M, Sharma A. Structural analysis of ABC-family periplasmic zinc binding protein provides new insights into mechanism of ligand uptake and release. J Mol Biol 2007;367(4):970–82.

[99] Nardini M, Lang DA, Liebeton K, Jaeger K-E, Dijkstra BW. Crystal structure of pseudomonas aeruginosa lipase in the open conformation. The prototype for family I.1 of bacterial lipases. J Biol Chem 2000;275(40):31219–25.

[100] Qiao S, Luo Q, Zhao Y, Zhang XC, Huang Y. Structural basis for lipopolysaccharide insertion in the bacterial outer membrane. Nature 2014;517(7507):108–11.

[101] Sukumar M, Rizo J, Wall M, Dreyfus LA, Kupersztoch YM, Gierasch LM. The structure of Escherichia coli heat-stable enterotoxin b by nuclear magnetic resonance and circular dichroism. Protein Sci 1995;4(9):1718–29.

[102] Tosi T, et al. Pilotin-secretin recognition in the type II secretion system of Klebsiella oxytoca. Mol Microbiol, 2011;82(6):1422–32.

[103] Lietzke SE, et al. The Refined Three-Dimensional Structure of Pectate Lyase E from Erwinia chrysanthemi at 2.2 A Resolution. Plant Physiol 1996;111(1):73–92.

[104] Brun E, Moriaud F, Gans P, Blackledge MJ, Barras F, Marion D. Solution structure of the cellulose-binding domain of the endoglucanase Z secreted by Erwinia chrysanthemi. Biochemistry 1997;36(51):16074–86.

[105] Zavialov AV, Berglund J, Pudney AF, Fooks LJ, Ibrahim TM, MacIntyre S, et al. Structure and biogenesis of the capsular F1 antigen from Yersinia pestis: preserved folding energy drives fiber formation. Cell 2003;113(5):587–96.

[106] David G, Blondeau K, Schiltz M, Penel S, Lewit-Bentley A. YodA from Escherichia coli is a metal-binding, lipocalin-like protein. J Biol Chem 2003;278(44):43728–35.

[107] Leverrier P, Declercq J-P, Denoncin K, Vertommen D, Hiniker A, Cho S-H, et al. Crystal structure of the outer membrane protein RcsF, a new substrate for the periplasmic protein-disulfide isomerase DsbC. J Biol Chem 2011;286(19):16734–42.

[108] Kishida H, Unzai S, Roper DI, Lloyd A, Park S-Y, Tame JRH. Crystal structure of penicillin binding protein 4 (dacB) from Escherichia coli, both in the native form and covalently linked to various antibiotics. Biochemistry 2006;45(3):783–92.

[109] Nickitenko AV, Trakhanov S, Quiocho FA. 2 A resolution structure of DppA, a periplasmic dipeptide transport/chemosensory receptor. Biochemistry 1995;34(51):16585–95.

[110] Thayer MM, Flaherty KM, McKay DB. Three-dimensional structure of the elastase of Pseudomonas aeruginosa at 1.5-A resolution. J Biol Chem 1991;266(5):2864–71.

[111] Brown NG et al. Structural and biochemical evidence that a TEM-1 beta-lactamase N170G active site mutant acts via substrate-assisted catalysis. J Biol Chem 2009;284(48):33703–12.

[112] Ramboarina S, Fernandes PJ, Daniell S, Islam S, Simpson P, Frankel G, et al. Structure of the bundle-forming pilus from enteropathogenic Escherichia coli. J Biol Chem 2005;280(48):40252–60.

[113] Kim EE, Wyckoff HW. Reaction mechanism of alkaline phosphatase based on crystal structures. Two-metal ion catalysis. J Mol Biol 1991;218(2):449–64.

[114] Ishida H, Garcia-Herrero A, Vogel HJ. The periplasmic domain of Escherichia coli outer membrane protein A can undergo a localized temperature dependent structural transition. Biochim Biophys Acta 2014;1838(12):3014–24.

[115] Spreter T, Yip CK, Sanowar S, André I, Kimbrough TG, Vuckovic M, et al. A conserved structural motif mediates formation of the periplasmic rings in the type III secretion system. Nat Struct Mol Biol 2009;16(5):468–76.

[116] Yang JC, et al. Solution structure and domain architecture of the divisome protein FtsN. Mol Microbiol, 2004;52(3):651–60.

[117] Craig L, Taylor RK, Pique ME, Adair BD, Arvai AS, Singh M, et al. Type IV pilin structure and assembly: X-ray and EM analyses of Vibrio cholerae toxin-coregulated pilus and Pseudomonas aeruginosa PAK pilin. Mol Cell 2003;11(5):1139–50.

[118] Laskowski RA, Chistyakov VV, Thornton JM. PDBsum more: new summaries and analyses of the known 3D structures of proteins and nucleic acids. Nucleic Acids Res 2005;33(Database issue):D266–8.

[119] Regad L, Guyon F, Maupetit J, Tufféry P, Camproux AC. A Hidden Markov Model applied to the protein 3D structure analysis. Comput Stat Data Anal 2008;52(6):3198–207.

[120] Unger R, Harel D, Wherland S, Sussman JL. A 3D building blocks approach to analyzing and predicting structure of proteins. Protein Struct Funct Genet 1989;5(4):355–73.

[121] Dasgupta B, Dey S, Chakrabarti P. Water and side-chain embedded π-turns. Biopolymers 2014;101(5):441–53.

[122] Dhar J, Chakrabarti P. Defining the loop structures in proteins based on composite β-turn mimics. Protein Eng Des Sel 2015;28(6):153–61.

[123] Fernandez-Fuentes N et al. Classification of common functional loops of kinase super-families. Proteins: Struct., Funct., Bioinf 2004;56(3):539–55.

[124] Thomsen MCF, Nielsen M. Seq2Logo: a method for construction and visualization of amino acid binding motifs and sequence profiles including sequence weighting, pseudo counts and two-sided representation of amino acid enrichment and depletion. Nucleic Acids Res 2012;40(Web Server issue):W281–W287.

[125] Smith RP et al. Targeting Bacterial Dsb Proteins for the Development of Anti-Virulence Agents. Molecules 2016;21(7).

[126] Dhouib R, Vagenas D, Hong Y, Verderosa AD, Martin JL, Heras B, et al. Antivirulence DsbA inhibitors attenuate Salmonella enterica serovar Typhimurium fitness without detectable resistance. FASEB Bioadv 2021;3(4):231–42.

[127] Adams LA, Sharma P, Mohanty B, Ilyichova OV, Mulcair MD, Williams ML, et al. Application of fragment-based screening to the design of inhibitors of Escherichia coli DsbA. Angew Chem Int Ed Engl 2015;54(7):2179–84.

[128] Duncan LF et al. The Fragment-Based Development of a Benzofuran Hit as a New Class of Escherichia coli DsbA Inhibitors. Molecules 2019;24(20).

[129] Bentley MR, Ilyichova OV, Wang G, Williams ML, Sharma G, Alwan WS, et al. Rapid Elaboration of Fragments into Leads by X-ray Crystallographic Screening of Parallel Chemical Libraries (REFiL(X)). J Med Chem 2020;63(13):6863–75.

[130] Duncan LF et al. Elaboration of a Benzofuran Scaffold and Evaluation of Binding Affinity and Inhibition of Escherichia coli DsbA: A Fragment-Based Drug Design Approach to Novel Antivirulence Compounds. Bioorg Med Chem 2021:116315.